Sabatino, A.D. and Clement, R. and Heath, M.R. and McKee, D. (2015) Use of ocean colour remote sensing to monitor sea surface suspended sediments. In: TeraWatt Position Papers. Marine Alliance for Science and Technology Scotland (MASTS), St Andrews, pp. 129-140. ISBN 978-0-9934256-0-8 ,

USE OF OCEAN COLOUR REMOTE SENSING TO MONITOR SEA SURFACE SUSPENDED SEDIMENTS

06

A.D. Sabatino[1], R. Clement[2], M.R. Heath[1] and D. McKee[2]

1 DEPARTMENT OF MATHEMATICS AND STATISTICS,
UNIVERSITY OF STRATHCLYDE, 16 RICHMOND STREET, GLASGOW, G1 1XQ

2 DEPARTMENT OF PHYSICS,
UNIVERSITY OF STRATHCLYDE, 16 RICHMOND STREET, GLASGOW, G1 1XQ

JULY 2015: REVISION 1

back to contents

06/1 INTRODUCTION

Ocean colour remote sensing (OCRS) from satellite platforms has revolutionised our ability to monitor the interplay of physical and biogeochemical processes in surface waters of the ocean. Since the launch of SeaWiFS in 1996, a continuous time series of OCRS data has been accumulated from a series of satellite sensors giving near daily global coverage. These sensors measure top of atmosphere (TOA) spectral radiance which is corrected for atmospheric effects (~80% of the measured signal in the blue – Gordon 1978) to give water leaving radiances. From these purely optical signals, it is possible to derive a wide range of higher level products such as chlorophyll concentration, diffuse attenuation coefficients, photosynthetically available radiation (PAR) and a wide range of inherent optical properties (IOPs) to name but a few.

In terms of surface area and primary productivity, the global ocean is heavily dominated by deep, oceanic waters, where the optical properties are driven by phytoplankton, associated dissolved organics and water itself. It is little surprise then that early standard OCRS products were developed for optimal performance over these globally significant regions. Standard chlorophyll algorithms were developed using changes in blue-green reflectance ratios (e.g. O'Reilley et al., 1998) that can be related to the effect of changing concentrations of microscopic scale (1µm-200µm) phytoplankton (Kirk,1983) forming blooms that can stretch for thousands of km. More recently, attention has shifted to economically important coastal regions where, for example, harmful algal blooms have potential to cause significant societal and economic impact. OCRS algorithms have been developed to specifically aid in the monitoring of both toxic species e.g. *Karenia brevis* in the Gulf of Mexico (Stumpf et al., 2003), and also to monitor for extreme eutrophication events where excessive levels of phytoplankton cause the reduction of oxygen dissolved in the water column (hypoxia) leading to animal mortality (e.g. Mallin et al., 2006).

The optically complex nature of coastal waters, more generally, presents a particular problem for OCRS applications in these regions. Shallow shelf seas and other inshore waters are subject to the influence of sediment resuspension and freshwater discharge bringing additional loads of coloured dissolved organic materials (CDOM). This results in multiple, independently varying, optically significant components, each of which influences the water leaving radiance spectrum making interpretation of spectral changes significantly more difficult. Many studies have demonstrated the breakdown in performance of standard algorithms (e.g. Chl, McKee et al. 2007) in optically complex coastal waters.

In this paper we will focus on the effect of suspended sediment on optical properties of the water column. Suspended sediment has long been known to influence light penetration (Gordon and McCluney, 1975) which can limit primary production and also contribute to hypoxia (Greig et al., 2005). There is interest in monitoring sediment concentration for coastal erosion applications and various OCRS algorithms have been developed that exploit the relatively strong backscattering properties of sediment. For example, Doxaran et al. (2002) successfully presented a sediment algorithm for the highly turbid Gironde estuary. More recently a radiative transfer approach was used to refine this type of approach to incorporate the potential impact of other materials on the red reflectance values that support sediment algorithms (Neil et al., 2011). This algorithm provides estimates of maximum and minimum sediment load concentrations assuming reasonable potential ranges of Chl and CDOM for coastal waters. The aim of this paper is to determine the extent to which the Neil et al. algorithm, which was developed for Irish Sea waters, can be applied to data collected in the North Sea. The ultimate goal is to assess the potential for using OCRS data to monitor suspended sediment concentrations in coastal waters, with monitoring marine turbine arrays an obvious and potentially important application.

back to contents

06/2 OCEAN COLOUR REMOTE SENSING: FUNDAMENTAL CONCEPTS

06/2.1 WHAT DOES AN OCEAN COLOUR SATELLITE MEASURE?

Ocean colour is given by the spectral reflectance R at the sea surface for a given wavelength λ. This radiance reflectance, R, can be related to two inherent optical properties of the water column, the absorption $a(\lambda)$ and the backscattering $b_b(\lambda)$ (Sathyendranath et al., 1989).

$$R = f(a, b_b) \quad (1)$$

where the back scattering coefficient can be expressed as:

$$b_b = \int_{\pi/2}^{\pi} \beta(\theta) \sin\theta \, d\theta \quad (2)$$

and $\beta(\theta)$ is the volume scattering function at the angle θ. However, what OCRS satellites actually measure is the radiance at the top of the atmosphere, $L_t(\lambda)$, which includes photons scattered from within the sea, the sea surface and by aerosols and molecules in the atmosphere. The TOA radiance can be expressed as (Chen and Lu, 2009):

$$L_t(\lambda) = L_r(\lambda) + L_a(\lambda) + L_{ra}(\lambda) + T(\lambda)L_g(\lambda) + L_b(\lambda) + t(\lambda)L_{wc}(\lambda) + t(\lambda)(1-w)L_w(\lambda) \quad (3)$$

where the terms in the equation are:

- $L_r(\lambda)$ Rayleigh scattering radiance.
- $L_a(\lambda)$ Aerosol scattering radiance.
- $L_{ra}(\lambda)$ Multiple scattering between Rayleigh and aerosol radiances.
- $T(\lambda)$ Direct transmittance of the atmosphere or Beam Transmittance.
- $L_g(\lambda)$ Contribution from specular reflection of direct sunlight from the sea surface (sun glitter).
- $L_b(\lambda)$ Radiance from the bottom of the water.
- $t(\lambda)$ Diffuse transmittance between sea surface and sensor.
- $L_{wc}(\lambda)$ Contribution from sunlight and skylight reflecting by wave white capping.
- w Covering rate of whitecaps
- $L_w(\lambda)$ Water-leaving radiance.

By carefully constraining sun-sensor angles, view angles and by making a number of reasonable assumptions (Gordon and Wang, 1992; 1994a; Robinson et al., 2000), it is possible to simplify Eq 3 to:

$$L_t(\lambda) = L_r(\lambda) + L_a(\lambda) + t(\lambda)L_w(\lambda) \quad (4)$$

The reflectance and the radiance are related by:

$$L_t(\lambda) = \frac{R(\lambda)F_0(\lambda)\cos\theta_0}{\pi} \quad (5)$$

where $L_t(\lambda)$ is the total radiance received by the sensor, F_0 is the extra-terrestrial solar irradiance at a wavelength λ and θ_0 is the solar zenith angle. Given this relationship, it is possible to express Eq 4 in terms of reflectance rather than radiance as follows:

$$R_t(\lambda) = R_r(\lambda) + R_a(\lambda) + t(\lambda)R_w(\lambda) \quad (6)$$

in which the R_w term takes in account of corrections due to whitecapping, gas absorption, glitter and multiple scattering (Ruddick et al., 2000):

$$R_w(\lambda) = \frac{R_c(\lambda) - R_{am}(\lambda)}{t(\lambda)} \quad (7)$$

where R_c is the Rayleigh corrected reflectance, that can be written (Goyens et al., 2013):

$$R_c(\lambda) = R_t(\lambda) - R_r(\lambda) - t_v(\lambda)R_{wc}(\lambda) \quad (8)$$

while R_{am} is the multiple scattering term and is defined as:

$$R_{am}(\lambda) = R_a(\lambda) + R_{ra}(\lambda) \quad (9)$$

The TOA radiance signal is heavily dominated by the contributions from atmospheric scattering (~80%). For algorithms that require accurate estimates of water leaving radiance or surface remote sensing reflectance, it is therefore essential that an appropriate atmospheric correction is performed.

06/2.2 ATMOSPHERIC CORRECTION (AC)

Early atmospheric correction algorithms assumed that the water-leaving radiance term (L_w) was zero for wavelengths in the near-infrared (NIR). The so-called 'black pixel' approximation was based on the idea that absorption by water was sufficiently strong at NIR wavelengths that photons entering the water would not be reflected back. If true, equation (7) would reduce to:

$$R_{am}(NIR) = R_C(NIR) \quad (10)$$

With the implication that the multiple scattering term for NIR wavelengths is equal to the Rayleigh corrected reflectance, allowing selection of a suitable aerosol model that could be extrapolated to visible wavelengths in order to complete the correction.

However the black pixel approximation is not valid for turbid coastal waters where strong backscattering from suspended sediments is sufficient to ensure that some NIR photons that enter the water column are reflected, resulting in a non-zero water leaving radiance in the NIR (Ruddick et al, 2000; Dall'Olmo et al., 2005). Various AC approaches have been developed for operations over turbid waters. The improved NIR model for standard NASA ocean colour data processing uses an iterative approach that begins by assuming zero water leaving radiance in the NIR, generating a visible L_w spectrum that is used to estimate an initial Chl value. This data is fed into a bio-optical model that gives a new value of L_w in the NIR and the algorithm iterates until the chlorophyll concentration is within 20% of the previous iteration, up to a maximum of four iterations, after which it terminates (Bailey et al., 2010; Stumpf et al., 2003). This algorithm was designed for operation in open ocean and coastal waters dominated by phytoplankton, but is known to perform poorly in coastal waters where sediment contributes strongly to the water leaving radiance signal.

An alternative, the MUMM atmospheric correction algorithm (Ruddick et al., 2000) was specifically designed for operation over highly turbid coastal waters and is built on two main assumptions: 1) the atmosphere composition does not vary significantly spatially within a reasonably sized scene, and 2) total absorption in the NIR region is largely determined by pure water absorption, which is invariant. The algorithm allows the user to choose two calibration parameters: the aerosol reflectance ratio, ε, and the water leaving reflectance ratio, α, where these ratios are defined as:

$$\varepsilon^{(7,8)} \equiv \frac{R_{am}^{(7)}}{R_{am}^{(8)}} \quad (11)$$

$$\alpha \equiv \frac{a_w^{(8)}}{a_w^{(7)}} \quad (12)$$

and $R_{am}^{(i)}$ is the multiple-scattering aerosol reflectance at waveband i, and $a_w(i)$ is the pure water absorption coefficient at waveband i. Wavebands 7 and 8 for MODIS correspond to wavelengths of 748 and 869 nm respectively, in NIR region. These parameters are used to select an appropriate aerosol model for extrapolation into the visible.

06/2.3 AEROSOL MODELS

Having used the first part of the AC procedure to determine R_{am} in the NIR region, and using this to establish ε, the two closest aerosol models are chosen from a look-up table. Various aerosol models have been proposed (Antoine and Morel, 2011; Gohin et al., 2002; Gordon and Wang, 1994b; Shettle and Fenn, 1979; Wang, 2000):

- Oceanic: This model has the lowest value of ε of all the models available in SeaDAS.
- Tropospheric: This model has no oceanic contributions. It represents the particles that are present above the boundary layer, that are not as easily affected by local sources. And has a very high value of ε compared to the other models.
- Maritime: 99% of the particles in this model have tropospheric characteristics, and 1% oceanic. Refraction and particle radius depend on the relative humidity. The value of ε for this model is close to 1.

- Coastal: 99.5% of the particles in this model have tropospheric characteristics, and 0.5% oceanic. Refraction and particle radius depend on the relative humidity. The value of ε for this model is typically quite high.

Each of these models depends on the wavelength and relative humidity. Having selected an appropriate aerosol model, the atmospheric correction process is completed by using the aerosol model to extrapolate NIR atmospheric signals into the visible where they can be subtracted from the TOA signal, leaving the desired water-leaving signal as the residual.

06/2.4 OCRS DATA SOURCE AND PROCESSING TOOLS

The Ocean Biology Processing Group (OBPG) at NASA's Goddard Space Flight Center maintains a database of OCRS data (Ocean Color Web) for a series of sensors going all the way back to CZCS (starts 1978, with gap from 1986 when CZCS stopped to 1996 when SeaWiFS started). NASA provides free access to the historic time series. The SeaWiFS Data Analysis System (SeaDAS) software was developed by NASA (Fu et al., 1998) for processing data from this source.

06/3 SUSPENDED SEDIMENT ALGORITHM

The remote sensing reflectance, $R_{rs}(\lambda)$, is defined as (Mobley, 1994):

$$R_{rs}(\lambda) = \frac{L_u(\lambda)}{E_d(\lambda)} \quad (13)$$

where L_u is the upwelling radiance above the surface and E_d is the downwelling irradiance above the surface, both at a given wavelength λ. L_u can be related to the water-leaving radiance, L_w, as follows (Austin, 1980):

$$L_w = 0.544\, L_u \quad (14)$$

As discussed above, R_{rs} can also be related to the ratio of backscattering to absorption (Kirk, 1994):

$$R_{rs} \approx \kappa \frac{b_b}{a} \quad (15)$$

where κ is not exactly a constant of proportionality, but can be treated as such for conditions relevant for satellite ocean colour remote sensing.

Total backscattering and absorption coefficients can be modelled as consisting of components due to water, phytoplankton (Chl) and mineral suspended solids (MSS), with absorption including an additional term due to CDOM which is assumed to be non-scattering (Mobley, 1999; Kirk, 1994). R_{rs} can therefore be related to optical constituents via:

$$R_{rs} \approx \frac{b^*_{b\,W} + b^*_{b\,MSS} MSS + b^*_{b\,CHL} CHL}{a_W + a^*_{MSS} MSS + a^*_{CHL} CHL + a^*_{CDOM} CDOM} \quad (16)$$

where the a^* and $b_b{}^*$ parameters are concentration-specific IOPs. Absorption at red / NIR wavelengths is dominated by the component due to water for most natural waters, except for extremely turbid waters where the component due to MSS can become significant or even dominate. High levels of MSS in turbid coastal waters results in MSS dominating the backscattering signal. Neil et al. (2011) performed a radiative transfer simulation study with realistic values of specific IOPs for UK coastal waters (McKee and Cunningham, 2006) and demonstrated the well known relationship between red remote sensing reflectance and MSS for moderately turbid waters. Importantly, however, they also demonstrated the potential impact of Chl and $CDOM$ on the relationship between $R_{rs}667$ and MSS, leading to development of an algorithm that estimates upper and lower bounds for MSS for a given $R_{rs}667$ value. These bounds are based upon reasonable assumptions of the maximum impact of other constituents for typical UK coastal water concentration ranges. The resulting relationships were found:

$$MSS_{(u)} = 26014 \times (R_{rs}667)^2 + 916 \times (R_{rs}667) - 0.13 \quad (17)$$

$$MSS_{(l)} = 2508 \times (R_{rs}667)^2 + 768 \times (R_{rs}667) - 0.77 \quad (18)$$

A subsequent study highlighted the possibility of using this algorithm to investigate physical processes such as the onset and break down of stratification in shallow shelf seas using ocean colour remote sensing (Neil et al., 2012).

06/4 ALGORITHM VALIDATION AND APPLICATION FOR THE EAST COAST OF SCOTLAND

The Neil et al. (2011) sediment algorithm was developed using SIOPs obtained in the Irish Sea and other west coast areas. Before it can be routinely applied to other areas, it is necessary to perform a local validation to ensure that it provides reasonable estimates for the region of interest where there is potential for SIOPs to be significantly different. The algorithm was applied to MODIS data downloaded directly from NASA GSFC and processed in SeaDAS using the improved NIR and MUMM atmospheric correction algorithms (separately). All available clear sky images for the east coast of Scotland between 2008 and 2011 were identified, downloaded and processed, with a 5 x 5 pixel array centred on the main Marine Scotland sampling site off Stonehaven selected for subsequent analysis. OCRS sediment concentrations were compared with data from vertical profiles of turbidity (Formazine Turbidity Units (FTU), proportional to SPM ($g.m^{-3}$)) which were measured at 0.5m depth intervals and up to weekly intervals over the period 2008-2011 (Bresnan et al. 2008, Serpetti et al. 2012, Serpetti 2012; Heath et al., subm. a, Heath et al., subm b.). Figures 6.1 and 6.2 show preliminary results which indicate that there is good correspondence between OCRS estimates of sediment concentration using the Neil et al. algorithm and in situ measurements of turbidity (Clement 2014). The choice of atmospheric correction does have an impact on individual OCRS data points, but the overall picture is broadly similar. Further analysis is required to determine which AC approach provides the best match with in situ data (work currently in progress).

Figures 6.3-6.6 show seasonally averaged upper bound MSS distributions for the east coast of Scotland. Sediment levels are generally low for offshore waters, with levels decreasing further in summer and autumn when thermal stratification occurs and tidally stirred sediment does not reach surface waters. High sediment concentrations are restricted to a narrow region close to shore in autumn – spring, but even this diminishes significantly in summer. The tidal basin at Montrose appears to be a candidate source for enhanced local sediment concentrations. Figures 6.7 and 6.8 show the difference in upper bound MSS estimates for choice of atmospheric correction algorithm by season. In both cases the maximum difference is approximately 2 g m^{-3} with the spring data showing greater variation than autumn. Although these differences are not massive, there is clearly an imperative to establish an optimal data processing scheme that may require an adaptive approach that varies by season or even on a pixel-by-pixel basis.

06/5 CONCLUSIONS

This study has presented a preliminary demonstration of ability to observe spatial and temporal patterns of variability in sediment distributions from OCRS data. Further work is required to refine the data processing steps and to establish robust error budgets for the OCRS sediment products. In associated TeraWatt position papers, Heath et al. (submitted a and b) propose an algorithm based on in situ data to predict suspended sediments from a set of physical variables. OCRS data could be useful for assimilation into and validating this model. The next step will be to prepare monthly mean and seasonal maps of sediment distributions for the Pentland Firth area to support establishment of baseline properties for areas where tidal stream renewables arrays will be located. It is anticipated that these may prove useful in demonstrating the impact (or otherwise) of such arrays on sediment loading and associated light field parameters.

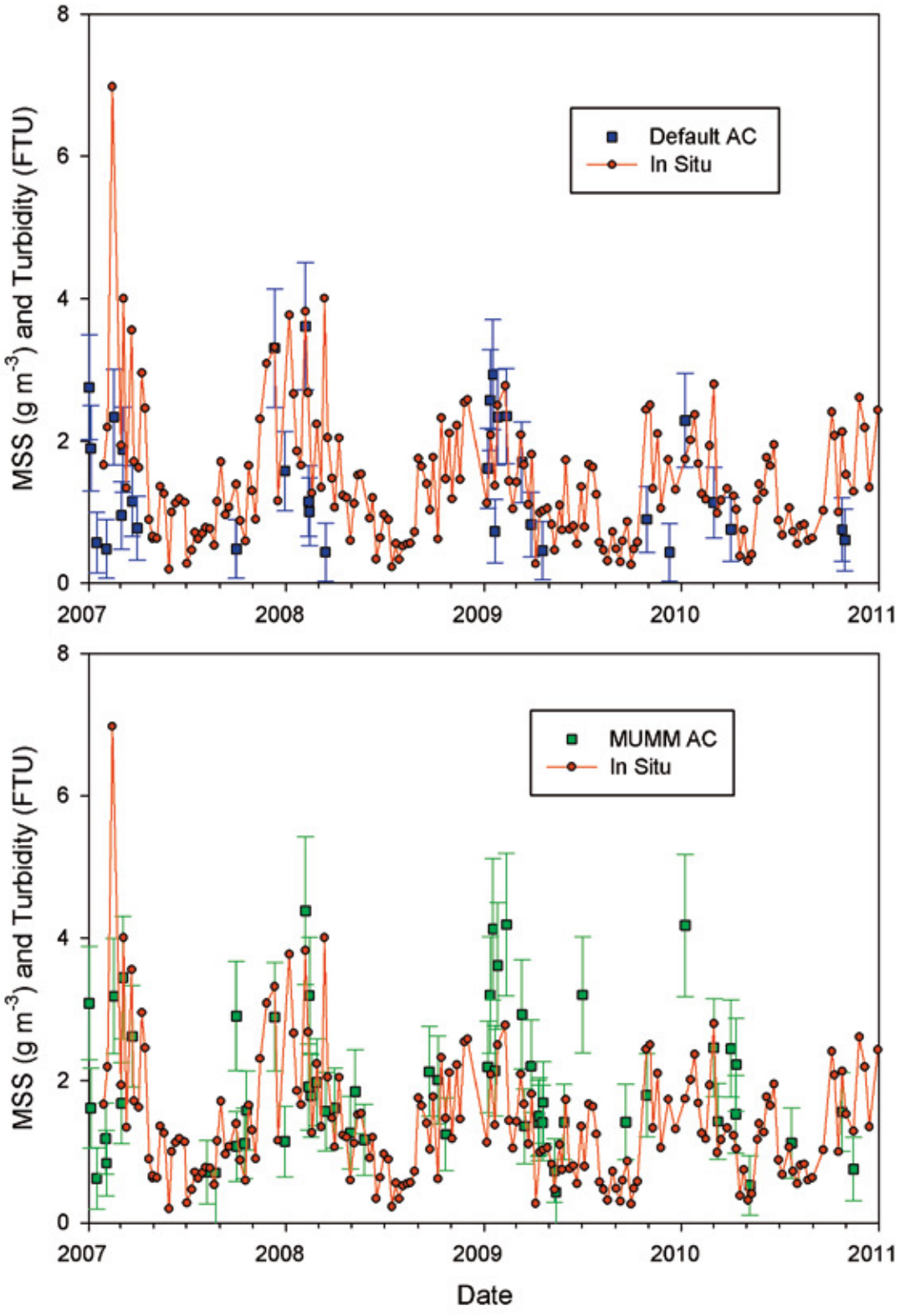

Fig 6.1 & 6.2 Time series data for the different AC algorithms applied. The top time series (Figure 6.1) shows the satellite-derived MSS levels from using the default AC algorithm, represented by the error bars to show the upper and lower bounds of these levels. The bottom time series (Figure 6.2) has the MUMM AC algorithm applied to the MSS data, where it is represented by green error bars to show the upper and lower bounds. Figures adapted from Clement (2014).

back to contents

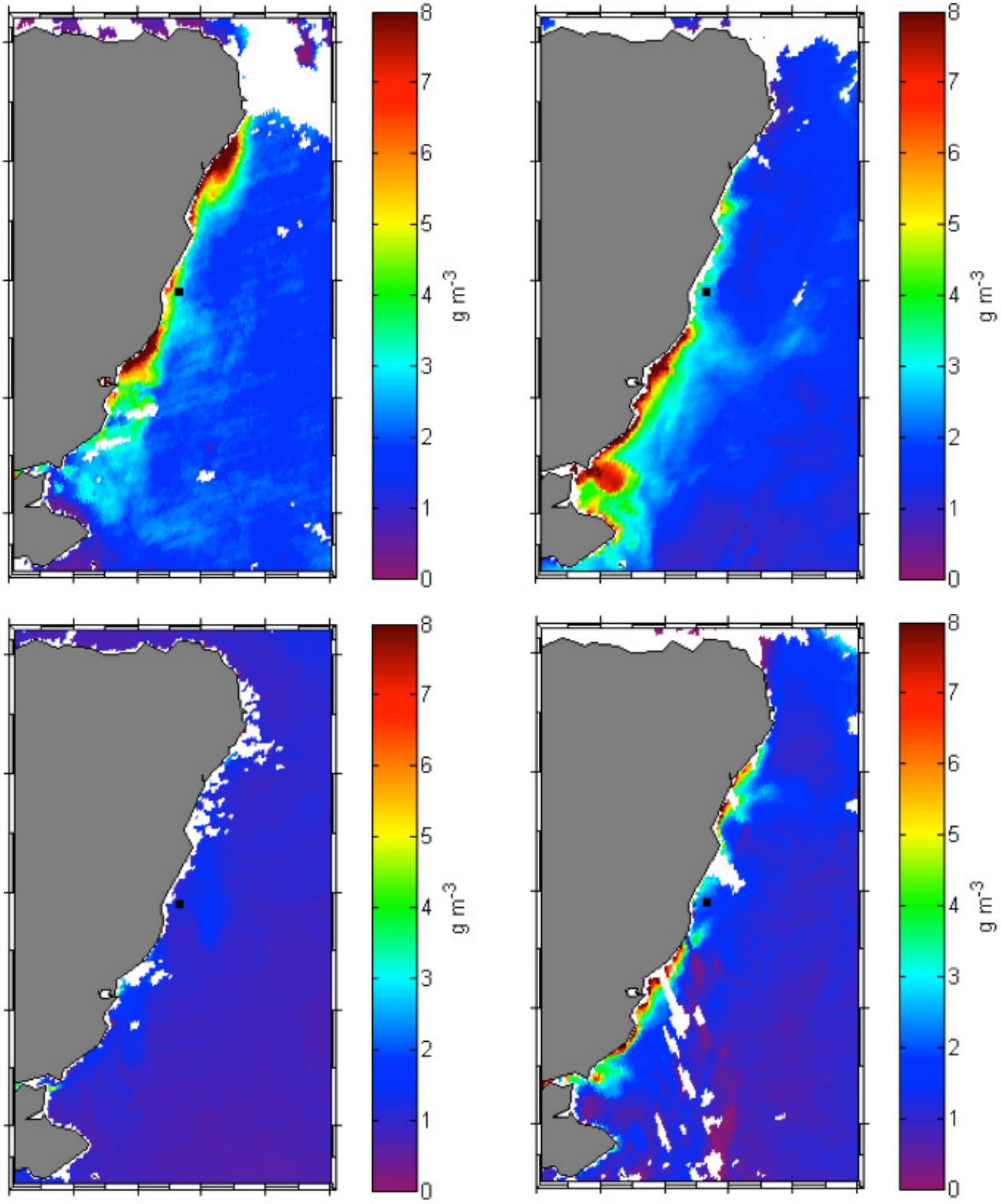

Fig 6.3 - 6.6 Seasonal variation in the MSS upper level.
Figure 6.3 Top left – winter (02/01/2007),
Figure 6.4 Top right – spring (29/03/2009),
Figure 6.5 Bottom left – summer (08/08/07) and
Figure 6.6 Bottom right – autumn (25/10/10).
These were produced with the MUMM AC algorithm (average ε used = 0.9825). Figures from Clement (2014).

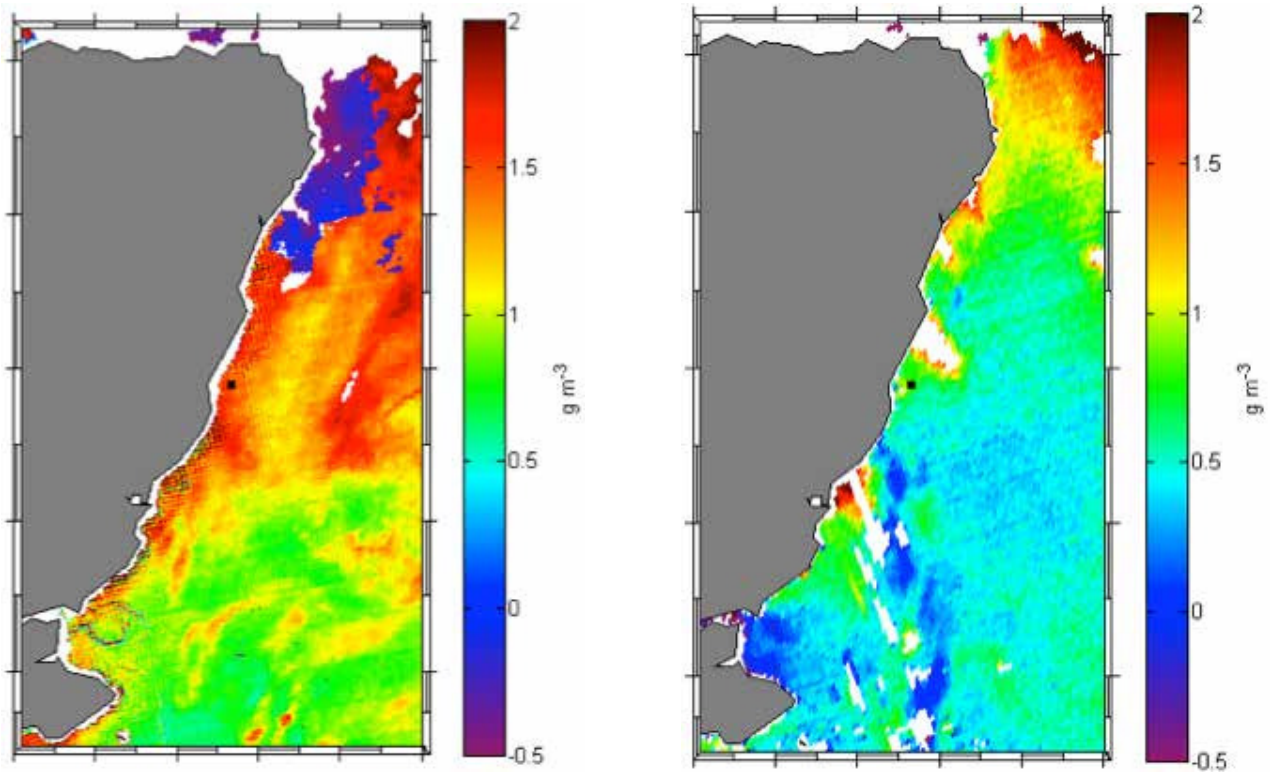

Fig 6.7 & 6.8 Difference in MSS level for the upper bound, for the MUMM and default AC algorithms.
Figure 6.7: Left – spring difference (29/03/2009)
Figure 6.8: Right – autumn difference (25/10/10). Figure from Clement (2014).

06/6 REFERENCES

Antoine, D., Morel, A. (2011). *MERIS ATBD 2.7 - Atmospheric Correction of the MERIS observations Over Ocean Case 1 waters*. [report] Laboratoire D'Océanographie De Villefranche.

Austin, R. (1980). *Gulf of Mexico, ocean-color surface-truth measurements.*Boundary-Layer Meteorology, 18 (3), pp. 269-285.

Bailey, S. W., Franz, B. A., Werdell, P. J. (2010). *Estimation of near-infrared water-leaving reflectance for satellite ocean color data processing.* Optics Express, 18 (7), pp. 7521-7527.

Bresnan, E., Hay, S., Hughes, S.L., Fraser, S., Rasmussen, J., Webster, L., Slesser, G., Dunn, J., Heath, M.R. 2008. Seasonal and interannual variation in the phytoplankton community in the north east of Scotland. Journal of Sea Research 61, 17-25.

Chen, X., Lu, Z. (2009). *Remote sensing of water environment.* In: Li, D., Shan, J., Gong, J. eds. (2009). Geospatial technology for earth observation. New York: Springer, pp. 431-471.

Clement, R. (2014). *Mapping Marine Sediments from Space for Renewable Energy Applications.* PH450 Project Report.

Dall'Olmo, G., Gitelson, A. A., Rundquist, D. C., Leavitt, B., Barrow, T., Holz, J. C. (2005). *Assessing the potential of SeaWiFS and MODIS for estimating chlorophyll concentration in turbid productive waters using red and near-infrared bands.* Remote Sensing of Environment, 96(2), 176-187.

Doxaran, D., Froidefond, J. M., Lavender, S., Castaing, P. (2002). *Spectral signature of highly turbid waters: Application with SPOT data to quantify suspended particulate matter concentrations.* Remote sensing of Environment, 81(1), 149-161.

Fu, G., Baith, K. S., McClain, C. R. (1998). *SeaDAS: The SeaWiFS data analysis system.* In Proceedings of the 4th Pacific Ocean remote sensing conference, Qingdao, China (pp. 28-31).

Gohin, F., Druon, J., Lampert, L. (2002). *A five channel chlorophyll concentration algorithm applied to SeaWiFS data processed by SeaDAS in coastal waters.* International Journal Of Remote Sensing, 23 (8), pp. 1639-1661.

Gordon, H. R., McCluney, W. R. (1975). *Estimation of the sunlight penetration in the sea for remote sensing.* Applied Optics, 14, 413 – 416.

Gordon, H. R. (1978). *Removal of atmospheric effects from satellite imagery of the oceans.* Applied Optics, 17, 1631-1636.

Gordon, H. R., Wang, M. (1994a). *Influence of oceanic whitecaps on atmospheric correction of ocean-color sensors.* Applied Optics, 33 (33), pp. 7754-7763.

Gordon, H. R. , Wang, M. (1994b). *Retrieval of water-leaving radiance and aerosol optical thickness over the oceans with SeaWiFS: a preliminary algorithm.* Applied Optics, 33 (3), pp. 443-452.

Gordon, H. R., Wang, M. (1992). *Surface-roughness considerations for atmospheric correction of ocean color sensors. I: The Rayleigh-scattering component*. Applied Optics, 31 (21), pp. 4247-4260.

Goyens, C., Jamet, C., Schroeder, T. (2013). *Evaluation of four atmospheric correction algorithms for MODIS-Aqua images over contrasted coastal waters.* Remote Sensing Of Environment, 131, pp. 63-75.

Greig, S. M., Sear, D. A., Carling, P. A. (2005). *The impact of fine sediment accumulation on the survival of incubating salmon progeny: implications for sediment management.* Science of the Total Environment, 344(1), 241-258.

Heath, M.R., Sabatino, A.D., O'Hara Murray, R.B. (submitted a). *Scoping the impact of tidal and wave energy extraction on suspended sediment concentrations and underwater light climate.*

Heath, M.R., Sabatino, A.D., McCaig, C., O'Hara Murray, R.B. (submitted b). *Modelling spatial and temporal patterns of turbidity off the east coast of Scotland.*

Kirk, J. T. O. (1983). *Light and photosynthesis in aquatic ecosystems.* Cambridge [England]: Cambridge University Press.

Kirk, J. T. O. (1994). *Light and photosynthesis in aquatic ecosystems (2nd edition).* Cambridge [England]: Cambridge University Press.

Mallin, M. A., Johnson, V. L., Ensign, S. H., MacPherson, T. A. (2006). *Factors contributing to hypoxia in rivers, lakes, and streams.* Limnology and Oceanography, 51(1part2), 690-701.

McKee, D., Cunningham, A. (2006). *Identification and characterization of two optical water types from in situ inherent optical properties and seawater constituents.* Estuarine, Coastal and Shelf Science, 68, 305–316.

McKee, D., Cunningham, A., Wright, D., Hay, L. (2007). *Potential impacts of nonalgal materials on water-leaving Sun induced chlorophyll fluorescence signals in coastal waters.* Applied Optics, 46(31), 7720-7729.

Mobley, C. D. (1994). *Light and Water.* San Diego: Academic Press.

Mobley, C. D. (1999). *Estimation of the remote-sensing reflectance from above-surface measurements.* Applied Optics, 38, 7442–7455.

Neil, C., Cunningham, A., McKee, D. (2011). *Relationships between suspended mineral concentrations and red-waveband reflectances in moderately turbid shelf seas.* Remote Sensing of Environment, 115(12), 3719-3730.

Neil, C., Cunningham, A., McKee, D., Polton, J. A. (2012). *Remote sensing of seasonal stratification d ynamics in the southern Irish Sea.* Remote Sensing of Environment, 127, 288-297.

O'Reilley, J. E., Maritorena, S., Mitchell, B. G., Siegel, D. A., Carder, K. L., Garver, S. A., Kahru, M., McClain, C. (1998). *Ocean color chlorophyll algorithm for SeaWiFS.* Journal of Geophysical Research, 103 (C11), 24937 – 24953.

Robinson, W. D., Schmidt, G. M., McClain, C. R. & Werdell, P. J. (2000). *Changes Made in the Operational SeaWiFS Processing.* In: Hooker, S. B. & Firestone, E. R. eds. (2000). NASA Tech. Memo. 2000-206892. Vol 10. Greenbelt, Maryland: NASA Goddard Space Flight Center, pp12-28.

back to contents

Ruddick, K. G., Ovidio, F., Rijkeboar, M. (2000). *Atmospheric correction of SeaWiFS imagery over turbid coastal waters.* Applied Optics, 39 (6), pp. 897-912.

Sathyendranath, S., Prieur, L., Morel, A. (1989). *A three-component model of ocean colour and its application to remote sensing of phytoplankton pigments in coastal waters.* International Journal of Remote Sensing, 10(8), 1373-1394.

Serpetti, N. 2012. *Modelling and mapping the physical and biogeochemical properties of sediments on the North Sea coastal waters.* PhD Thesis, University of Aberdeen. 249pp.

Serpetti, N., Heath, M., Rose, M. and Witte, U. (2012). *Mapping organic matter in seabed sediments off the north-east coast of Scotland (UK) from acoustic reflectance data*. Hydrobiologia 680, 265–284.

Shettle, E. P. , Fenn, R. W. (1979). *Models for the aerosols of the lower atmosphere and the effects of humidity variations on their optical properties.*

Stumpf, R. P., Culver, M. E., Tester, P. A., Tomlinson, M., Kirkpatrick, G. J., Pederson, B. A., Truby, E., Ransibrahmanakul, V., Soracco, M. (2003). *Monitoring Karenia brevis blooms in the Gulf of Mexico using satellite ocean color imagery and other data.* Harmful Algae, 2(2), 147-160.

Wang, M. (2000). *The SeaWiFS atmospheric correction algorithm updates.*
Seawifs Postlaunch Calibration And Validation Analyses, Part, 1, pp. 57-63.